

Original Article

Cite this article: Grewal HS, Ahmad S, and Jin H. (2023) Dosimetric study of the interplay effect using three-dimensional motion phantom in proton pencil beam scanning treatment of moving thoracic tumours. *Journal of Radiotherapy in Practice*. 22(e11), 1–10. doi: [10.1017/S1460396921000479](https://doi.org/10.1017/S1460396921000479)

Received: 12 April 2021

Revised: 25 June 2021

Accepted: 13 July 2021


Key words:

interplay effect; pencil beam scanning; phantom study; respiratory-gated treatment; volumetric repainting

Author for correspondence:

Salahuddin Ahmad, Ph.D., Department of Radiation Oncology, University of Oklahoma Health Sciences Center, 800 NE 10th Street, SCC L 100, Oklahoma City, OK 73104, USA. E-mail: Salahuddin-ahmad@ouhsc.edu

Dosimetric study of the interplay effect using three-dimensional motion phantom in proton pencil beam scanning treatment of moving thoracic tumours

Hardev S. Grewal^{1,2}, Salahuddin Ahmad¹  and Hosang Jin³

¹Department of Radiation Oncology, University of Oklahoma Health Sciences Center, Oklahoma City, Ok, USA;

²Oklahoma Proton Center, Oklahoma City, OK, USA and ³Department of Radiation Oncology, Baylor Scott & White Health, Temple, TX, USA

Abstract

Aim: The dosimetric and clinical advantages offered by implementation of pencil beam scanning (PBS) proton therapy for moving thoracic tumours is hindered by interplay effect. The purpose of this study is to evaluate the impact of large proton beam spot size along with adaptive aperture (AA) and various motion mitigation techniques on the interplay effect for a range of motion amplitudes in a three-dimensional (3D) respiratory motion phantom.

Materials and Methods: Point doses using ionisation chamber (IC) and planner dose distributions with radiochromic film were compared against the corresponding treatment planning system (TPS) information. A 3D respiratory motion phantom was scanned either for static or 4D computed tomographic (CT) technique for 6-, 10- and 14-mm motion amplitudes in SI direction. For free breathing (FB) treatment, a tumour was contoured on maximum intensity projection scan and an average scan was used for treatment planning. Each FB treatment was delivered with one, three and five volumetric repainting (VRs). Three phases (CT40–60%) were extracted from the 4D-CT scans of each motion amplitude for the respiratory-gated treatment and were used for the treatment planning and delivery. All treatment plans were made using AA and robustly optimised with 5-mm set-up and 3.5% density uncertainty. A total of 26 treatment plans were delivered to IC and film using static, dynamic and respiratory-gated treatments combinations. A percent dose difference between IC and TPS for the point dose and gamma indices for film–TPS planner dose comparison was used.

Results: The dose profile of film and TPS for the static phantom matched well, and percent dose difference between IC and TPS was 0.4%. The percent dose difference for all the gated treatments were below 3.0% except 14-mm motion amplitude-gated treatment. The gamma passing rate was more than 95% for film–TPS comparison for all gated treatment for the investigated gamma acceptance criteria. For FB treatments, the percent dose difference for 6-, 10- and 14-mm motion amplitude was 1.4%, –2.7% and –4.1%, respectively. As the number of VR increased, the percent difference between measured and calculated values decreased. The gamma passing rate met the required tolerance for different acceptance criteria except for the 14-mm motion amplitude FB treatment.

Conclusion: The PBS technique for the FB thoracic treatments up to 10-mm motion amplitude can be implemented with an acceptable accuracy using large proton beam spot size, AA and robust optimisation. The impact of the interplay effect can be reduced with VR and respiratory-gated treatment and extend the treatable tumour motion amplitude.

Introduction

Proton therapy has demonstrated dosimetric advantages over photon therapy for the treatment of thoracic tumours.^{1,2} Proton therapy with pencil beam scanning (PBS) technique has been more susceptible to the interplay effect³ which refers to deviation of delivered dose distributions from the planned distributions due to combined effects of inter-field tumour motion and spot scanning. The initial clinical data regarding the treatment of thoracic tumours primarily came from passively scattered proton therapy (PSPT). However, treatment plans made using the PSPT technique were relatively robust against the interplay effect which lacks intensity modulation and the ability to adjust modulation width for various thicknesses of tumour resulting in additional dose to nearby critical structures.⁴ Motion mitigation techniques reduce the impact of the interplay effect for PBS, thus lowering the critical organ doses and aid in therapeutic dose escalation for tumours while maintaining critical organ doses.⁵

© The Author(s), 2021. Published by Cambridge University Press. This is an Open Access article, distributed under the terms of the Creative Commons Attribution licence (<http://creativecommons.org/licenses/by/4.0/>), which permits unrestricted re-use, distribution and reproduction, provided the original article is properly cited.

Table 1. Proton beam spot size measured in-air using a Lynx scintillation detector for a range of clinical energies used in this study for the compact proton therapy system

No	Range (g/cm ²)	Energy (MeV)	Spot size (1 σ mm)
1	1.1	33.0	17.4
2	1.7	42.5	16.3
3	2.3	50.8	15.6
4	2.9	58.0	14.9
5	3.6	64.7	14.6
6	4.2	70.8	14.1
7	4.8	76.6	13.5
8	5.4	82.1	13.2
9	6.0	87.4	12.7
10	6.6	92.3	12.3
11	7.3	97.1	12.0
12	7.9	101.7	11.6
13	8.5	106.3	11.4
14	9.1	110.5	11.0
15	9.7	114.8	10.6
16	10.6	120.2	10.4

The interplay effect depends on several factors including proton machine characteristics, tumour size, tumour location and the magnitude of motion of the tumour. Mevion (Littleton, MA) S250i with Hyperscan is a compact proton therapy system with a proton beam spot size substantially larger than the traditional systems. Table 1 shows the spot size measured at isocentre by a Lynx (IBA-Dosimetry, Schwarzenbruck, Germany) scintillation detector with a 10-cm air gap for central axis proton spots for a range of energies appropriate for this study. The system uses adaptive aperture (AA) to sharpen the lateral penumbra of the field which aids in reducing the dose to the critical structures located laterally. Clinically, it is very important to study the impact of the larger spot size along with the application of AA on the interplay effect for a range of motion amplitudes to identify the appropriate patient group for treatment with PBS. For PBS treatment, volumetric repainting (VR) and respiratory-gated treatment are among the recommended motion mitigation techniques for reducing dosimetric uncertainties caused by the interplay effect for large amplitude tumour motion.⁵ Both techniques tend to increase the overall treatment delivery time, a valuable resource in a single-room proton therapy system. Thus, it is vital that the dosimetric benefit provided by these techniques in conjunction with larger spot size and AA will be examined.

The use of the larger proton beam spot size and robust optimisation are parameters that can reduce the impact of the interplay effect. Grassberger et al.⁶ performed four-dimensional Monte Carlo (4D MC) simulations for ten patients by varying spot sizes to study the interplay effect. They reported that plans of large spot sizes ($\sigma \approx 13$ mm) were less sensitive to tumour motion and target dose homogeneity was decreased by a factor of 2.8 for those made

with small spot sizes ($\sigma \approx 3$ mm). Chang et al.⁵ proposed 4D computed tomographic (CT) imaging, robust optimisation and evaluation, active motion management and delivery techniques for consensus guidelines on behalf of proton therapy collaborative group (PTCOG) for implementing PBS for thoracic tumours. Active motion management and delivery techniques include breath-hold, gating, tracking, volumetric rescanning and layer rescanning. Results from anthropomorphic phantoms by Imaging and Radiation Oncology Core (IROC) showed that the lung phantom had the second worst mean dose agreement (≈ 0.96) for the thermoluminescence dosimeter (TLD) to treatment planning system (TPS) ratio.⁷ Zhang et al.⁸ reported that increasing spot spacing reduced the impact of the interplay effect, but reducing layer switching time for volumetric rescanning did not improve the plan quality. Wang et al.⁹ reported MC dose calculations agreed better than an analytical algorithm with measured dose on a moving anthropomorphic lung phantom with proton beam spot sizes from 3.6 mm to 4.8 mm.

To the best of our knowledge, there is no published work regarding the use of larger spot size with AA to study the interplay effect. Accordingly, the objective is to study the interplay effect by ionisation chamber (IC) and 2D film measurements for a range of tumour motions using a 3D motion phantom. Furthermore, the impact of the motion mitigation strategies such as VR and respiratory-gated treatment on the chamber dose and film dose distributions is evaluated.

Materials and Methods

Proton therapy system

Mevion S250i with Hyperscan and AA has a cyclotron on the rotating gantry and an energy modulation system (EMS) in the nozzle. The AA system consists of seven non-divergent nickel 200 alloy leaf pairs. The inner five and outer two leaf pairs are 0.5 cm and 2 cm wide, respectively. In the beam direction, all leaves are 10 cm in thickness. The system can trim the field edge spots on layer-by-layer basis, and this is known as dynamic collimation. The scanning speed is limited by mechanical motion of AA. A detailed description of the Mevion S250i with Hyperscan system is summarised elsewhere.^{10,11}

Motion phantom

The QUASAR (Modus, London, Ontario, CA) respiratory phantom is an oval-shaped acrylic body phantom with the following dimensions: 30 cm wide, 12 cm long and 20 cm in height. The rotation stage of the phantom allows 3D motion for insets to rotate as they translate in the superior–inferior (SI) direction. The phantom has two 8-cm diameter openings for the insert and drive units. Two cedar wood inserts were used in this study to mimic the lung tissue. One insert had an off-centre opening for the IC and the other insert allowed film to be sandwiched between two halves of the insert as shown in Figure 1. Both inserts had a 3-cm diameter spherical polystyrene tumour target.

Imaging and target contouring

The phantom was scanned on a GE Discovery CT scanner (GE Healthcare, Little Chalfont, UK) with film and chamber insert with static or 4D CT scans, for the latter ± 3 (6), ± 5 (10) and ± 7 (14)

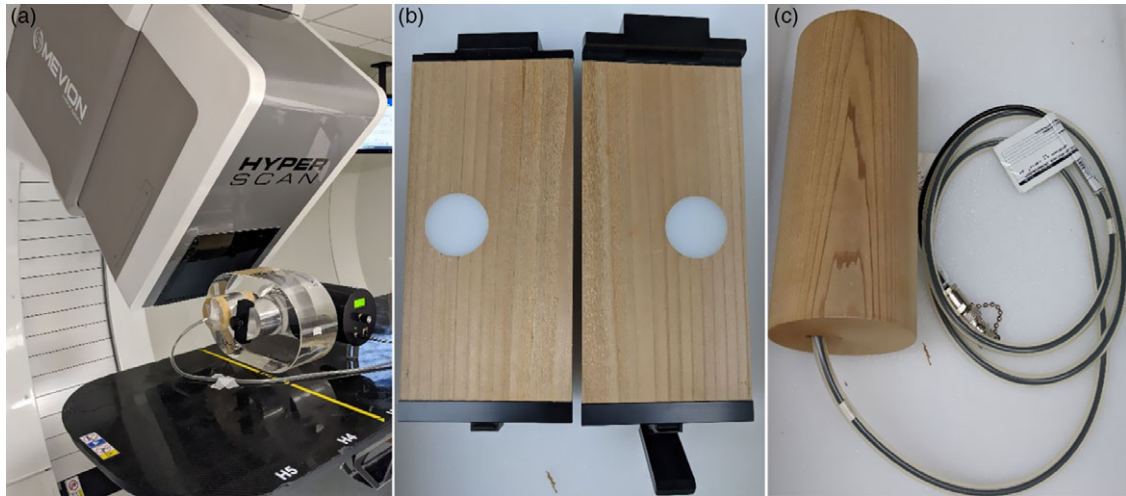


Figure 1. (a) Quasar motion phantom set-up on a treatment table in a Mevion's compact proton therapy system room; (b) cedar wood insert with 3-cm diameter offset target for film measurements; (c) cedar wood insert with compact CC04 chamber for a point dose measurement.

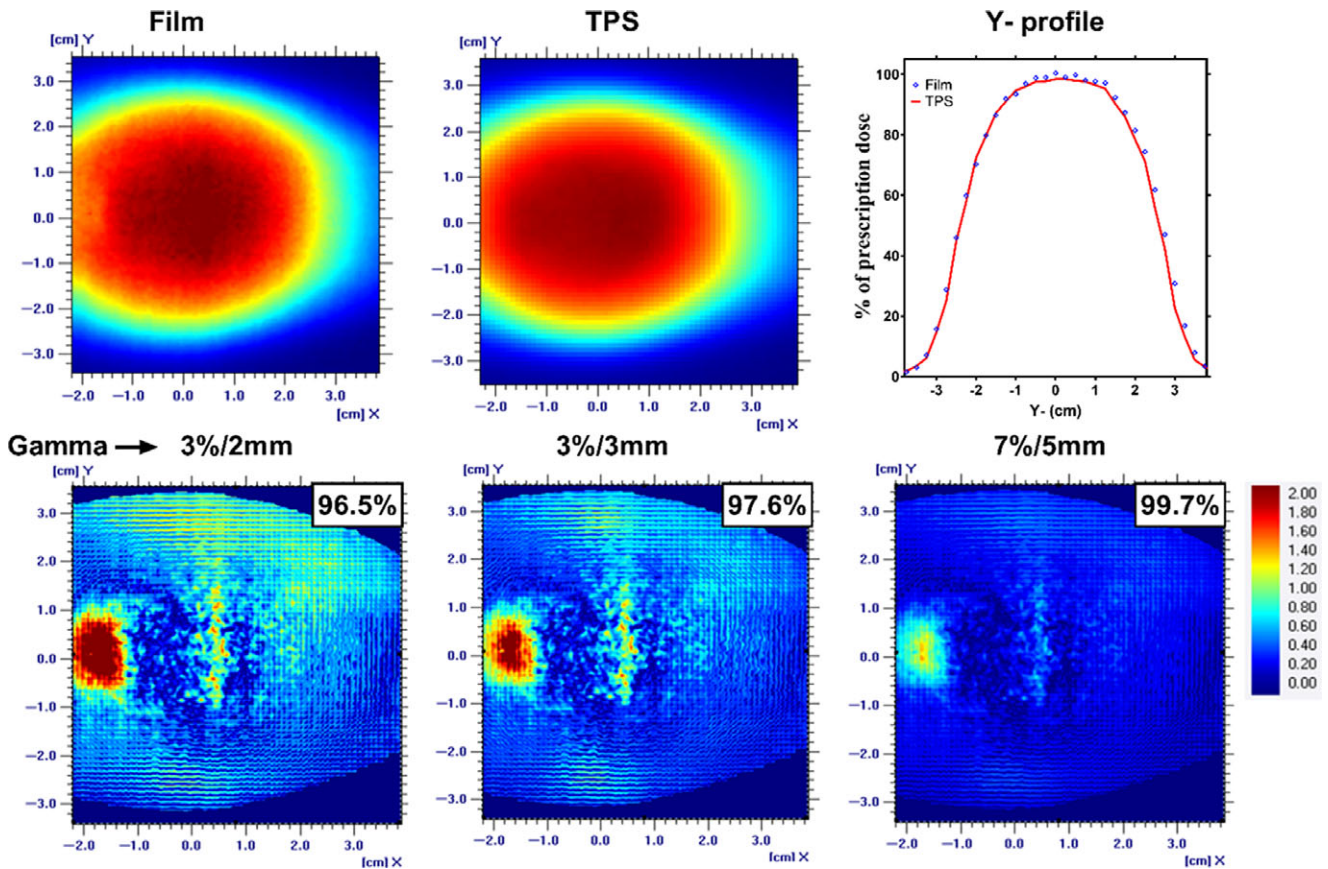


Figure 2. A planner view of the dose distribution along with the Y-axis profile for an EBT3 film and TPS for a static phantom condition. The gamma analysis with passing rate for the three acceptance criteria was also shown.

mm amplitude target motion were acquired. For free breathing (FB) 4D CT scans, a Real-time Position Management (RPM) system (Varian Medical Systems, Palo Alto, CA) was used to record the respiratory cycle information. The motion phantom used 15

breaths per minute to mimic the normal breathing rate of an adult patient. All scans were acquired with a slice thickness of 1.25 mm. The FB 4D CT scans was binned at ten equally spaced intervals with CT0% and CT50% representing maximum inhalation and

Table 2. Percent difference between chamber measurement and TPS dose for a static and respiratory-gated treatments. TPS dose was divided by 1.1 RBE factor to get in cGy

Motion technique	TPS (cGy)	Measurement (cGy)	% difference
Static	199.1	200.0	0.4
6-mm gated	199.8	200.0	0.1
10-mm gated	198.2	203.0	2.4
14-mm gated	201.3	209.0	3.8

exhalation, respectively. For FB plans, the maximum intensity projection (MIP) scans were used for internal gross tumour volume (IGTV) contouring and average scans for treatment planning. For respiratory-gated treatment, three phases from CT40–60% were extracted from binned 4D CT images. The tumour target was also contoured using MIP on all three phases to obtain the IGTV. The IGTV contour was mapped to the average scan from the three phases for the treatment planning. The same 40–60% gating window was used for respiratory-gated treatment delivery. The clinical target volume (CTV) was obtained by isotropic expansion of 5 mm from the IGTV.

Treatment planning

The RayStation TPS (RaySearch laboratories, Stockholm, Sweden; version 10A) was used to create individual treatment plans for IC and film measurements as per the scanning conditions. Each motion amplitude had 3 VR plans using one, three and five repainting for each IC and film measurement, where one repainting represents one pass of beam delivery in this study. Individual respiratory-gated treatment plans for each motion amplitude were made for both IC and film measurements. The IGTV was overridden by a density of 1.05 g/cm³ as recommended by the consensus guidelines for PBS thoracic proton therapy.⁵ Three gantry angles (G0, G45 and G120) were used with a single-field optimisation planning technique and AA to make treatment plans of 2 Gy (RBE) prescription dose per fraction. The MC algorithms were used for the optimisation and final dose calculations with 10,000 ion per spot and a statistical uncertainty of 0.5%, respectively. For optimisation, the treatment plans were made robustly with 5-mm set-up and 3.5% range (R) uncertainties for a total of 21 scenarios [7 (0, ±x, ±y, and ±z) × 3 (0, and ±R)]. Ninety-nine per cent of the CTV was covered by 100% of the prescription dose as normalisation criteria for all treatment plans.

Treatment delivery and analysis

A total of 26 treatment plans [(9 (3 VRs × 3 amplitudes) + 3 gated + 1 static) × 2 (IC and film)] were delivered to measure IC dose and film dose distribution. The beam-on time for these treatment plans were in the range of 60–110 s. The IC dose was measured with a compact chamber, CC04 (40 mm³, IBA dosimetry, Germany), which is well suited for small fields and high-dose gradients. The delivered dose distribution was evaluated with the GafChromic EBT3 (ISP, Wayne, NJ) films. The EBT3 films were stored for 24 h after irradiation in a dark and dry environment before scanned on the Epson 11,000 × L (Epson America,

Inc. Long Beach, CA) scanner with 48-bit colour and 150-dpi resolution. The optical density of the irradiated images was converted to the dose using calibration procedure with nine dose steps (0, 20, 70, 100, 200, 400, 600, 800 and 1000 cGy). The irradiation conditions for the calibration film were proton beam range of 16 g/cm², modulation 10 g/cm² and depth 11 cm in solid water. The OmniPro-ImRT software (IBA Dosimetry, Schwarzenbruck, Germany; version 1.6.009) was used to analyse measured and calculated planar dose distributions.

The percent difference between calculated/reference and measured IC dose was used to evaluate the difference between two doses with passing criteria of 3%. Film dose distributions for measured and calculated dose were analysed using the gamma analysis technique.¹² Three acceptance criteria of 3%/2 mm, 3%/3 mm and 7%/5 mm were applied in the gamma analysis. A 10% low-dose threshold was used in this analysis. The action limit of 90% gamma passing rate for the acceptance criteria of 3%/2 mm was chosen as per the recommendation of AAPM task group (TG) report of 218.¹³ The 3%/3 mm is the commonly used acceptance criteria in the clinic with the gamma passing rate of 95%. The relatively loose acceptance criteria of 7%/5 mm with the gamma passing rate of 85% was chosen from the IROC proton lung phantom credentialing criteria.

Results

Static phantom

The results from the static phantom represented motion free measurements and thus serve as a baseline for the motion study. The percent dose difference between chamber measurement and calculated TPS dose was 0.4% for the static phantom. Figure 2 shows well-matched y-axis (along the phantom motion direction) dose profile for both film and TPS measurement. The gamma passing rate was above the threshold used in this study with the percentage of 96.5%, 97.6% and 99.7% for the three acceptance criteria, 3%/2 mm, 3%/3 mm and 7%/5 mm, respectively, as shown in the Figure 2.

Respiratory-gated treatment

Table 2 shows the summary of the percent difference between chamber measurement and TPS-calculated dose for the respiratory-gated treatments. The gated treatment result for 14-mm motion amplitude failed to meet the 3% dose difference passing tolerance. But the results for the 6- and 10-mm motion amplitude-gated treatment were 0.1% and 2.4%, respectively. The dose profile and isodoses from the film measurement were in agreement with the TPS calculations for all the gated treatments as shown in Figure 3. The gamma passing rate was more than 95% for all the gated treatments even for the strictest acceptance criteria of 3%/2 mm (Figure 4).

FB treatment

The planned TPS coronal dose profile along the SI direction of the phantom travel was matched well with the EBT3 film measurement for 6- and 10-mm motion amplitude, but, for 14-mm motion amplitude, the measured dose profile especially in the

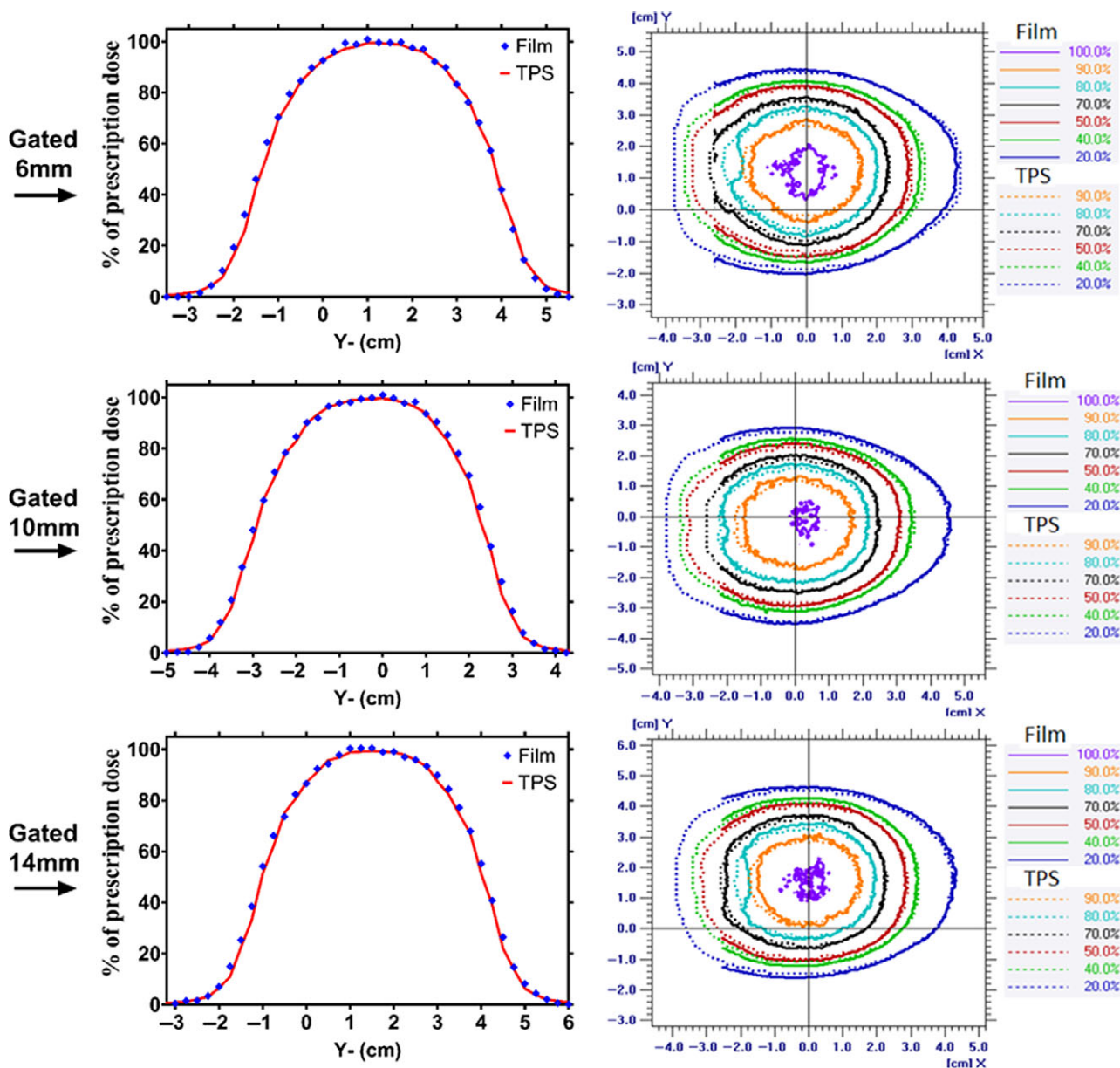


Figure 3. The dose profile along the superior–inferior (Y-axis) direction of the phantom travel and planner isodose alignment for 6-, 10-, and 14-mm respiratory-gated treatment for TPS and film measurement.

penumbra region did not match correctly with the reference distribution. Figures 5, 6 and 7 shows the gamma passing rate result for 6-, 10- and 14-mm motion amplitude FB treatment. The histogram analysis of the 6-mm amplitude FB motion shows gamma passing rate greater than 92.9% for 3%/2 mm and 95% for 3%/3 mm acceptance criteria (Figure 5: 1-VR). The gamma passing rate results for the 6-mm FB motion amplitude met the tolerance but lower than the corresponding 6-mm respiratory-gated treatment.

Similarly, the gamma passing rate results for 10-mm FB motion amplitude met the passing criteria set forth by the TG-218, clinical standard and IROC for their corresponding acceptance criteria of

3%/2 mm, 3%/3 mm and 7%/5 mm, respectively (Figure 6). The histogram analysis of the gamma for the 14-mm FB motion amplitude shows that it failed to meet the passing criteria for 3%/2 mm and 3%/3 mm acceptance criteria by getting 82.2% and 90.5%, respectively, gamma passing percentage (Figure 7: 1-VR). But 99.5% gamma passing rate was achieved with the relatively loose gamma acceptance criteria of IROC.

The results for the percent difference between chamber measurement and TPS-calculated dose for the 6-, 10- and 14-mm motion amplitude FB treatment were shown in Table 3. The FB treatment of 6- and 10-mm motion amplitude met the 3% absolute dose difference criteria 1.4% and -2.7%, respectively, for 1-VR.

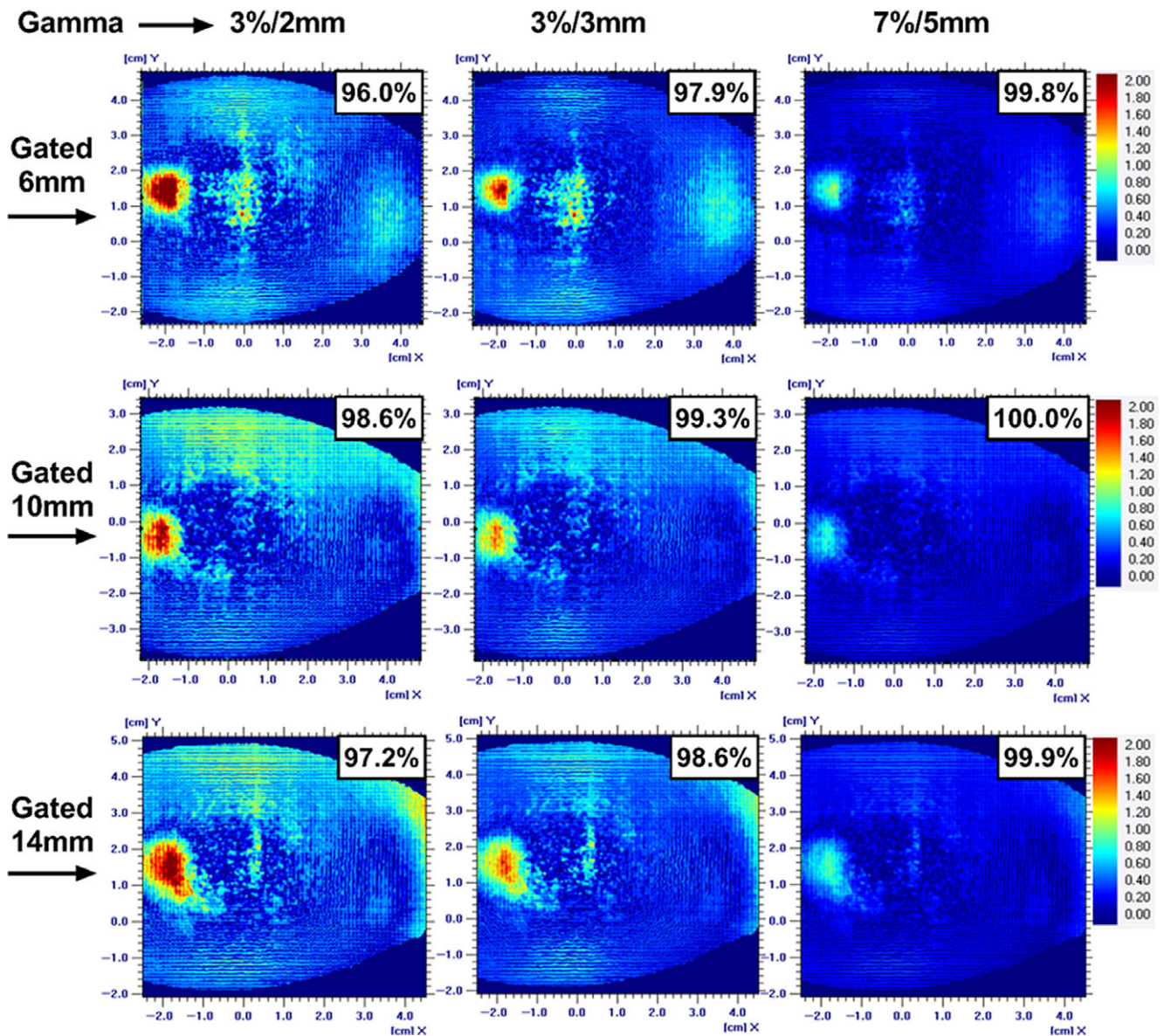


Figure 4. The gamma analysis on the coronal plane along with passing rate for 6-, 10-, and 14-mm respiratory-gated treatment for three gamma acceptance criteria.

The chamber measurements failed for the 14-mm motion amplitude at -4.1% .

VR evaluation

For the chamber measurements as the number of VR increased, the percent difference between measured and calculated dose decreased. The five VR for the 14-mm motion amplitude FB treatment resulted in percent dose difference of -2.6% , which failed with one VR. As the amplitude of the motion increased, the standard deviation which is a measure of the variability of the point dose among the VR for the IC measurements also increased. The standard deviations of the point dose among the VR (Table 3) for the 6-, 10- and 14-mm motion amplitude were 0.2% , 0.6% and 0.8% , respectively. The gamma passing rate also increased as the number of VR increased. The clinical standard gamma acceptance criteria of $3\%/3$ mm were satisfied when five

VRs were used for the 14-mm amplitude motion, which failed with one. The TG-218 criteria were not met by any of the VR deliveries.

Discussion

In this study, we quantitatively evaluated the interplay effect using 3D motion phantom for Mevion's S250i system for the range of tumour motion for FB and motion mitigation techniques such as VR and respiratory-gated treatments. The EMS consists of the 18 polycarbonate plates, and desired clinical energy is achieved by inserting a combination of these plates in the beam line. Due to multiple coulomb interactions of the proton beam with polycarbonate plates of the EMS in the nozzle, the proton beam spot size is larger than the other long beam line PBS delivery systems where EMS is located in the beam transport line.¹⁴

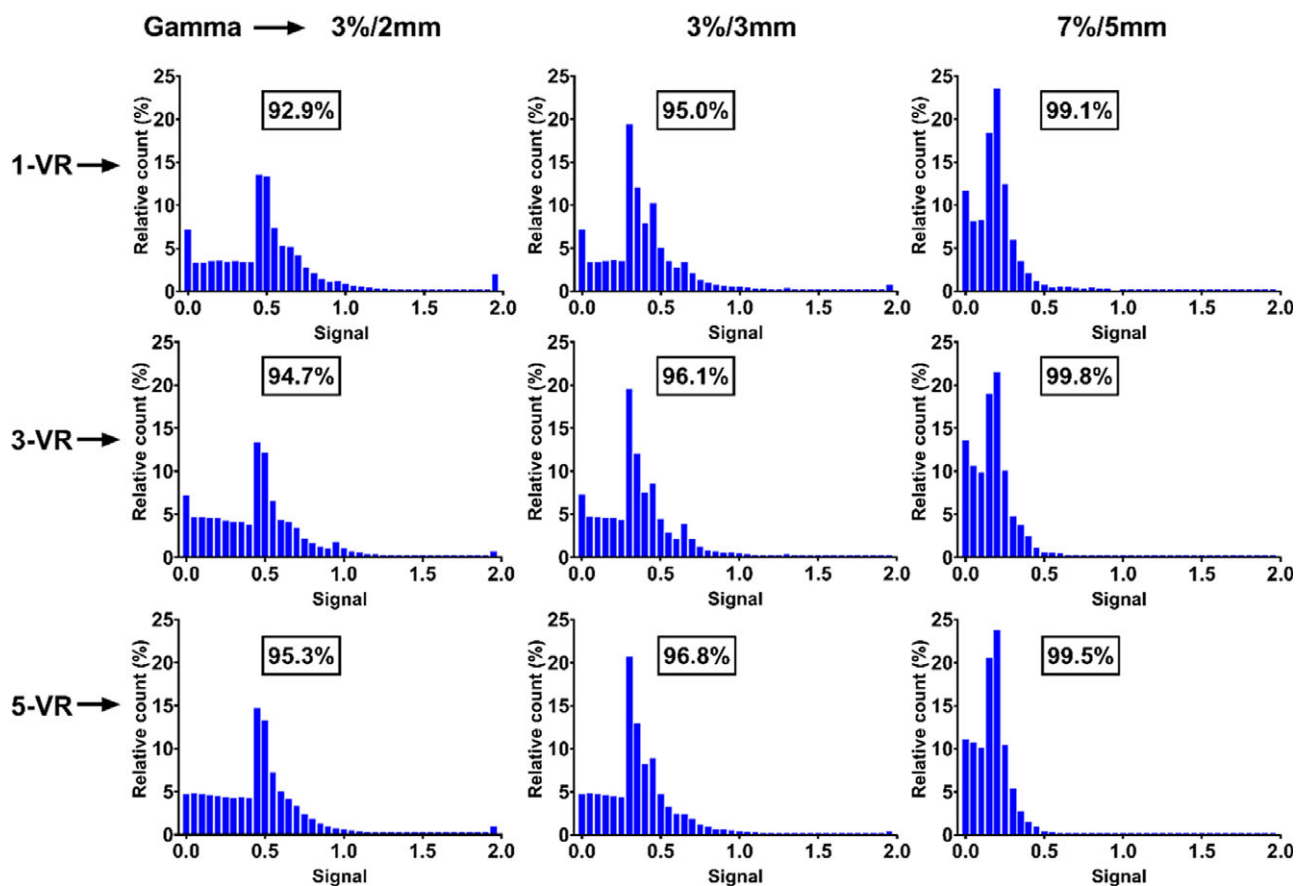


Figure 5. The histogram of the gamma analysis for three volume repainting and three gamma acceptance criteria for 6-mm free breathing motion.

The AA sharpens the proton field edge penumbra and keeps the proton beam central axis relatively unaffected at the cost of delaying beam delivery. The interplay effect study for lung cancer by Liu et al.¹⁵ reported significant dose sparing to critical structures such as heart and oesophagus with the small beam spot size (σ : 2–6 mm) as compared to large (σ : 6–15 mm). The extra doses to the critical structures were mainly due to large penumbra of the larger spot size. The AA mitigates the drawback of the large penumbra for the larger spot size by sharpening the field edge and led to dose sparing of the critical structures located laterally as reported by Grewal et al.¹⁶

For the respiratory-gated treatment, as the amplitude of the motion increased, the percent difference between measured and TPS-calculated dose increased as shown in Table 2. These results agreed with the qualitative behaviour observed by the Matsuura et al.¹⁷ for a phantom study with proton PBS-gated treatment. As compared to the FB treatment, respiratory-gated treatment reduces the treated volume. In this study, irradiated volume for 14-mm motion amplitude-gated treatment was 52% less than the corresponding FB treatment. This volume reduction was in range reported in the consensus guidelines by Chen et al.⁵

The VR appeared to be reducing the interplay effect. For each VR delivery, the standard deviation of the mean of the IC measurement increases as the breathing amplitude increases. We believe this is a result of the interplay effect which increases as

the motion amplitude increases. The general tendency for both IC and film measurements was better agreement between measured and TPS-calculated dose as the number of VR increased. For 14-mm FB motion amplitude profile and gamma histogram (Figure 7) show that as the number of VR increased the measured profile became better matched to the TPS-calculated profile and the gamma passing rate improved. It is believed that increasing the number of VR reduces the interplay effect by starting each VR randomly at different phases of the phantom motion.

Other components that may improve agreement between calculated and measured dose distributions for moving tumors include the use of robust optimization and MC algorithms for PBS dose calculations in heterogenous medium as reported by the Wang et al.⁹ MC-based proton dose calculation algorithms better predict regions of low dose and the shoulder region of the beam profile than the pencil beam algorithms. Robust optimisation helps in reducing the dose gradients in the target by taking into account the set-up and range uncertainties, which thus reduces the interplay effect.¹⁸

The present study has the following limitations. First, the EBT3 films suffer from quenching effects for the proton beam in the Bragg peak region.¹⁹ We tried to mitigate this effect by irradiating film from multiple directions (G0, G45 and G120) and film not parallel to the beam direction. The other strategies used were heavily weighted Bragg peaks (usually higher energies) that do not fall on to the film and overall energy spectrum

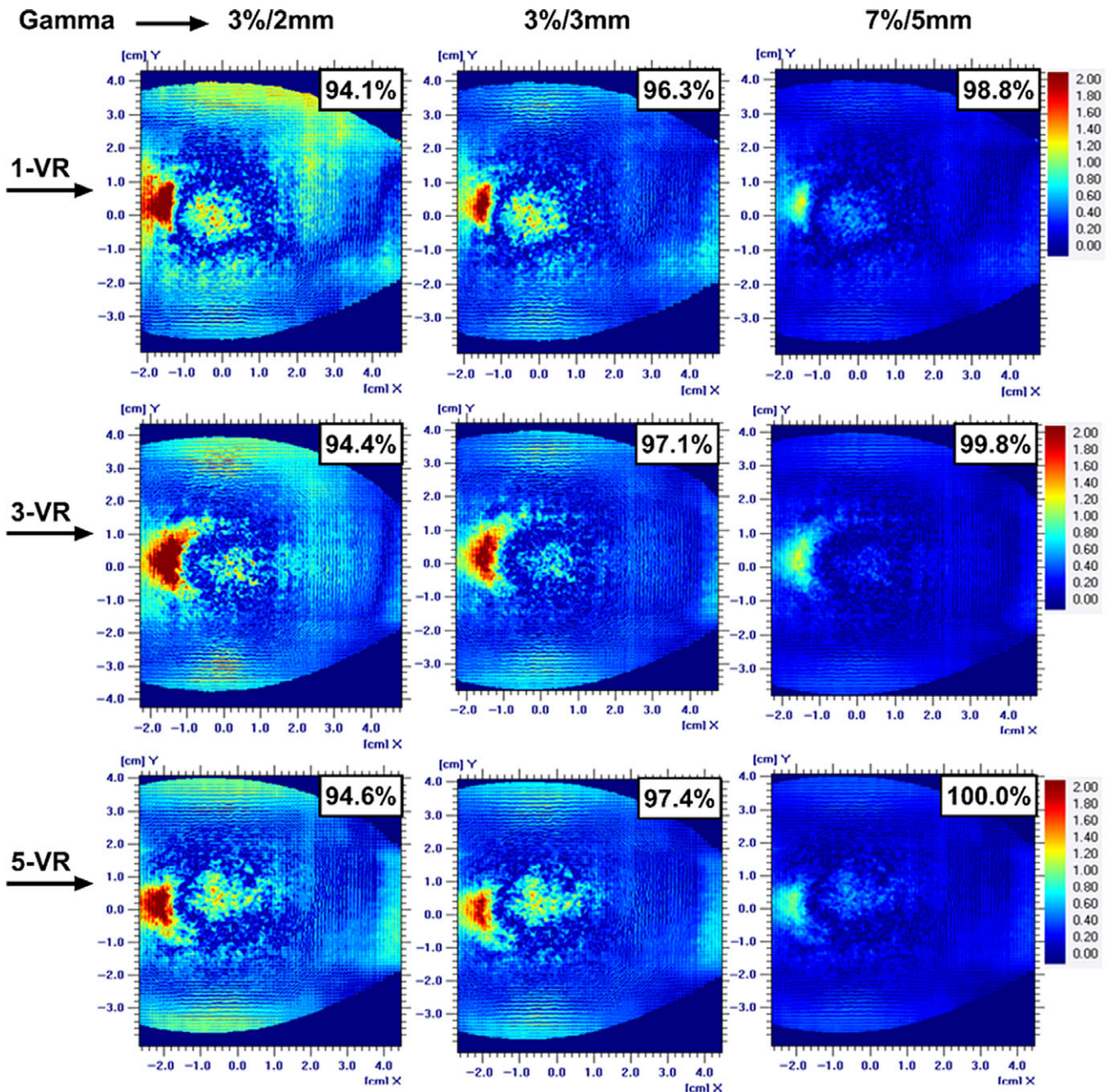


Figure 6. The gamma analysis for the 10-mm free breathing motion with different volumetric repainting techniques for the three gamma acceptance criteria.

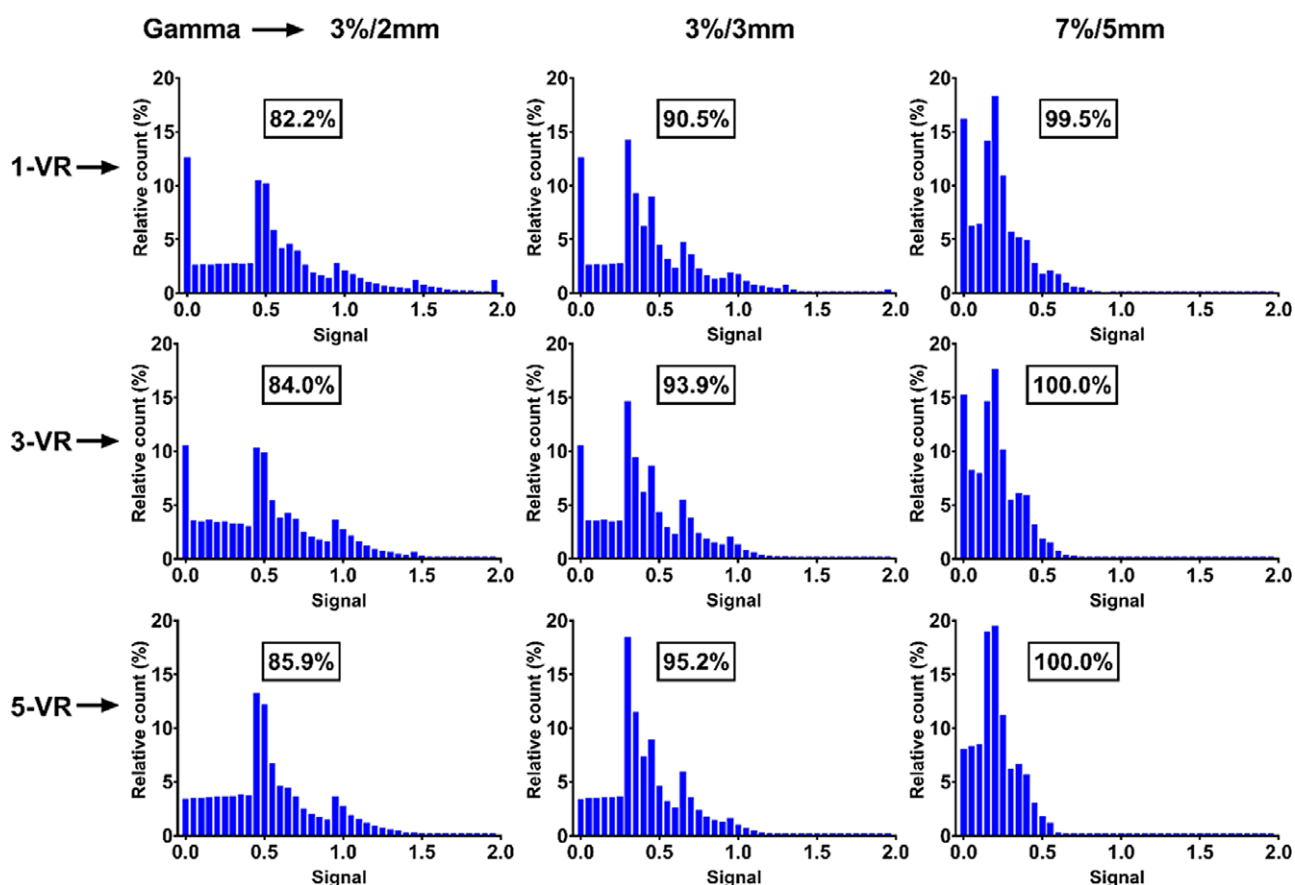
for film calibration should be similar to that of the measurement condition. Second, the phantom used a uniform breathing pattern. In clinical scenarios, a patient's breathing pattern may change during treatment. This may cause the uncertainty in the final delivered dose which is not predicted here. These uncertainties during actual treatment delivery may enhance the interplay effect, leading to larger dose discrepancies from treatment planning. Enhancement of this effect is related to variations in time of certain factors, such as longer respiratory period for example.²⁰ Third, we only studied the one size of the tumour, but the interplay effect can change with the size of the tumour and beam-on time. Finally, quantitative results presented in this study are machine-specific and a further study is needed to implement for different machine characteristics.

Conclusion

A proton PBS treatment for moving thoracic tumours holds great potential to reduce the normal tissue dose while maintaining the level of tumour control as the PSPT or photon-based treatments. An interplay effect depends on a number of factors, including beam spot size, spot spacing, tumour motion amplitude, size of the tumour, among others. In this study, we show that the PBS technique using large proton beam spot size, AA, robust optimisation and MC dose calculation algorithms for the FB thoracic treatments up to 10-mm tumour motion amplitude can be implemented with an acceptable accuracy. The impact of the interplay effect can be reduced with VR and respiratory-gated treatment which can extend the treatable tumour motion amplitude.

Table 3. Percent difference between chamber measurement and treatment planning system (TPS) dose for a free breathing (FB) and various volumetric repainting (VR)

Motion technique	No. of VR	TPS (cGy)	Measurement (cGy)	% difference
6-mm FB	1	196.2	199.0	1.4
	3	196.2	198.3	1.1
	5	196.2	198.2	1.0
10-mm FB	1	194.2	189.0	-2.7
	3	194.2	190.0	-2.2
	5	194.2	191.2	-1.5
14-mm FB	1	196.1	188.0	-4.1
	3	196.1	189.3	-3.5
	5	196.1	191.0	-2.6

**Figure 7.** The histogram representation of the gamma analysis for all volumetric repainting and gamma acceptance criteria for the 14-mm free breathing motion.

Acknowledgements. None.

References

- Chang JY, Zhang X, Wang X, et al. Significant reduction of normal tissue dose by proton radiotherapy compared with three-dimensional conformal or intensity-modulated radiation therapy in Stage I or Stage III non-small-cell lung cancer. *Int J Radiat Oncol Biol Phys* 2006; 65 (4): 1087–1096.
- Gomez D R, Gillin M, Liao Z, et al. Phase I study of dose escalation in hypofractionated proton beam therapy for non-small cell lung cancer. *Int J Radiat Oncol Biol Phys* 2013; 86 (4): 665–670.
- Kraus K M, Heath E, Oelfke U. Dosimetric consequences of tumour motion due to respiration for a scanned proton beam. *Phys Med Biol* 2011; 56 (20): 6563–6581.
- De Laney T F, Kooy H M, Ovid Technologies I. *Proton and Charged Particle Radiotherapy*. Philadelphia: Lippincott Williams & Wilkins, 2008.
- Chang JY, Zhang X, Knopf A, et al. Consensus guidelines for implementing Pencil-Beam scanning proton therapy for thoracic malignancies on behalf of the PTCOG thoracic and lymphoma subcommittee. *Int J Radiat Oncol Biol Phys* 2017; 99 (1): 41–50.
- Grassberger C, Dowdell S, Lomax A, et al. Motion interplay as a function of patient parameters and spot size in spot scanning proton therapy for lung cancer. *Int J Radiat Oncol Biol Phys* 2013; 86 (2): 380–386.

7. Taylor P A, Kry S F, Alvarez P, et al. Results from the imaging and radiation oncology core houston's anthropomorphic phantoms used for proton therapy clinical trial credentialing. *Int J Radiat Oncol Biol Phys* 2016; 95 (1): 242–248.
8. Zhang Y, Huth I, Wegner M, Weber D C, Lomax A J. An evaluation of rescanning technique for liver tumour treatments using a commercial PBS proton therapy system. *Radiother Oncol* 2016; 121 (2): 281–287.
9. Wang P, Tang S, Taylor P A, et al. Clinical examination of proton pencil beam scanning on a moving anthropomorphic lung phantom. *Med Dosim* 2019; 44 (2): 122–129.
10. Grewal H S, Ahmad S, Jin H. Performance evaluation of adaptive aperture's static and dynamic collimation in a compact pencil beam scanning proton therapy system: a dosimetric comparison study for multiple disease sites. *Med Dosim* 2021; 46 (2): 179–187.
11. Kang M, Pang D. Commissioning and beam characterization of the first gantry-mounted accelerator pencil beam scanning proton system. *Med Phys* 2020; 47 (8): 3496–3510.
12. Low D A, Harms W B, Mutic S, Purdy J A. A technique for the quantitative evaluation of dose distributions. *Med Phys* 1998; 25 (5): 656–661.
13. Miften M, Olch A, Mihailidis D, et al. Tolerance limits and methodologies for IMRT measurement-based verification QA: recommendations of AAPM Task Group No. 218. *Med Phys* 2018; 45 (4): e53–e83.
14. Saini J, Cao N, Bowen SR, et al. Clinical commissioning of a Pencil Beam scanning treatment planning system for proton therapy. *Int J Part Ther* 2016; 3 (1): 51–60.
15. Liu C, Schild S E, Chang J Y, et al. Impact of spot size and spacing on the quality of robustly optimized intensity modulated proton therapy plans for lung cancer. *Int J Radiat Oncol Biol Phys* 2018; 101 (2): 479–489.
16. Grewal H S, Ahmad S, Jin H. Characterization of penumbra sharpening and scattering by adaptive aperture for a compact pencil beam scanning proton therapy system. *Med Phys* 2021; 48 (4): 1508–1519.
17. Matsuura T, Miyamoto N, Shimizu S, et al. Integration of a real-time tumor monitoring system into gated proton spot-scanning beam therapy: an initial phantom study using patient tumor trajectory data. *Med Phys* 2013; 40 (7): 071729.
18. Wei L, Shang H, Jin F, Wang Y. Mitigation of the interplay effects of combining 4D robust with layer repainting techniques in proton-based SBRT for patients with early-stage non-small cell lung cancer. *Front Oncol* 2020; 10: 574605.
19. Khachonkham S, Dreindl R, Heilemann G, et al. Characteristic of EBT-XD and EBT3 radiochromic film dosimetry for photon and proton beams. *Phys Med Biol* 2018; 63 (6): 065007.
20. Pan C H, Shiau A C, Li K C, Hsu S H, Liang J A. The irregular breathing effect on target volume and coverage for lung stereotactic body radiotherapy. *J Appl Clin Med Phys* 2019; 20 (7): 109–120.